Vision Research 51 (2011) 867–880

Contents lists available at ScienceDirect

Vision Research

journal homepage: www.elsevier.com/locate/visres

Pursuing motion illusions: A realistic oculomotor framework for Bayesian inference

Amarender R. Bogadhi [a], Anna Montagnini [a], Pascal Mamassian [b], Laurent U. Perrinet [a], Guillaume S. Masson [a,*]

[a] Team DyVA, INCM, CNRS & Aix-Marseille Université, Marseille, France
[b] LPP, CNRS & Paris Descartes, Paris, France

ARTICLE INFO

Article history:
Received 26 June 2010
Received in revised form 15 October 2010
Available online 23 October 2010

Keywords:
Smooth pursuit eye movements
Motion perception
Aperture problem
Bayesian model
Temporal dynamics
Tracking error

ABSTRACT

Accuracy in estimating an object's global motion over time is not only affected by the noise in visual motion information but also by the spatial limitation of the local motion analyzers (aperture problem). Perceptual and oculomotor data demonstrate that during the initial stages of the motion information processing, 1D motion cues related to the object's edges have a dominating influence over the estimate of the object's global motion. However, during the later stages, 2D motion cues related to terminators (edge-endings) progressively take over, leading to a final correct estimate of the object's global motion. Here, we propose a recursive extension to the Bayesian framework for motion processing (Weiss, Simoncelli, & Adelson, 2002) cascaded with a model oculomotor plant to describe the dynamic integration of 1D and 2D motion information in the context of smooth pursuit eye movements. In the recurrent Bayesian framework, the prior defined in the velocity space is combined with the two independent measurement likelihood functions, representing edge-related and terminator-related information, respectively to obtain the posterior. The prior is updated with the posterior at the end of each iteration step. The maximum-a posteriori (MAP) of the posterior distribution at every time step is fed into the oculomotor plant to produce eye velocity responses that are compared to the human smooth pursuit data. The recurrent model was tuned with the variance of pursuit responses to either "pure" 1D or "pure" 2D motion. The oculomotor plant was tuned with an independent set of oculomotor data, including the effects of line length (i.e. stimulus energy) and directional anisotropies in the smooth pursuit responses. The model not only provides an accurate qualitative account of dynamic motion integration but also a quantitative account that is close to the smooth pursuit response across several conditions (three contrasts and three speeds) for two human subjects.

1. Introduction

Motion illusions help us to better understand how motion information is processed by the visual system. In particular, they illuminate how the brain processes ambiguous information to infer the most probable source from the external world (Kersten, Mamassian, & Yuille, 2004). The aperture problem, and its perceptual consequences, is one of the most investigated cases of motion illusions since it can be investigated at both perceptual, motor and neuronal levels (see Masson and Ilg (2010) for a collection of reviews). Motion sensitive cells in early visual stages have small receptive fields and, therefore, a limited access to the motion information present in the images. Neurons with receptive fields located at different positions along a simple moving stimulus such as a bar will provide different velocity measurements as illustrated in Fig. 1a. Consider two frames of a tilted line translating horizontally but seen through three small, circular apertures (locations 1–3). The translation vector in the 1st and 3rd apertures is unique as there is only one possible way to recover the translation of the line between the two frames, thanks to the two-dimensional (2D) profile of luminance information. Thus, motion recovered from the translation of these line-endings (also called features, terminators, or local 2D motion) is unambiguous, as illustrated by the small gaussian-like distribution of the most probable velocities in the (v_x, v_y) space, for a high signal-to-noise ratio (Lorenceau & Shiffrar, 1992; Pack, Hunter & Born, 2005). On the contrary, analyzing the translation of a one-dimensional luminance profile as seen in the 2nd aperture yields to an infinite number of possible velocity vectors. Such 1D motion is highly ambiguous (Movshon, Adelson, Gizzi, & Newsome, 1986) leading to the aperture problem. One can compute the 1D velocity likelihoods in the same (v_x, v_y) space, which under some assumptions about noise properties, would correspond to an elongated Gaussian distribution crossing an entire quadrant (Simoncelli, Adelson, & Heeger, 1991; Weiss et al., 2002). Understanding how purely horizontal motion of the entire

* Corresponding author. Address: Team DyVA, Institut de Neurosciences Cognitives de la Méditerranée, 31 Chemin Joseph Aiguier, 13402 Marseille cedex 20, France. Fax: +33 (0)4 91164498.
E-mail address: Guillaume.Masson@incm.cnrs-mrs.fr (G.S. Masson).

0042-6989/$ - see front matter © 2010 Elsevier Ltd. All rights reserved.
doi:10.1016/j.visres.2010.10.021

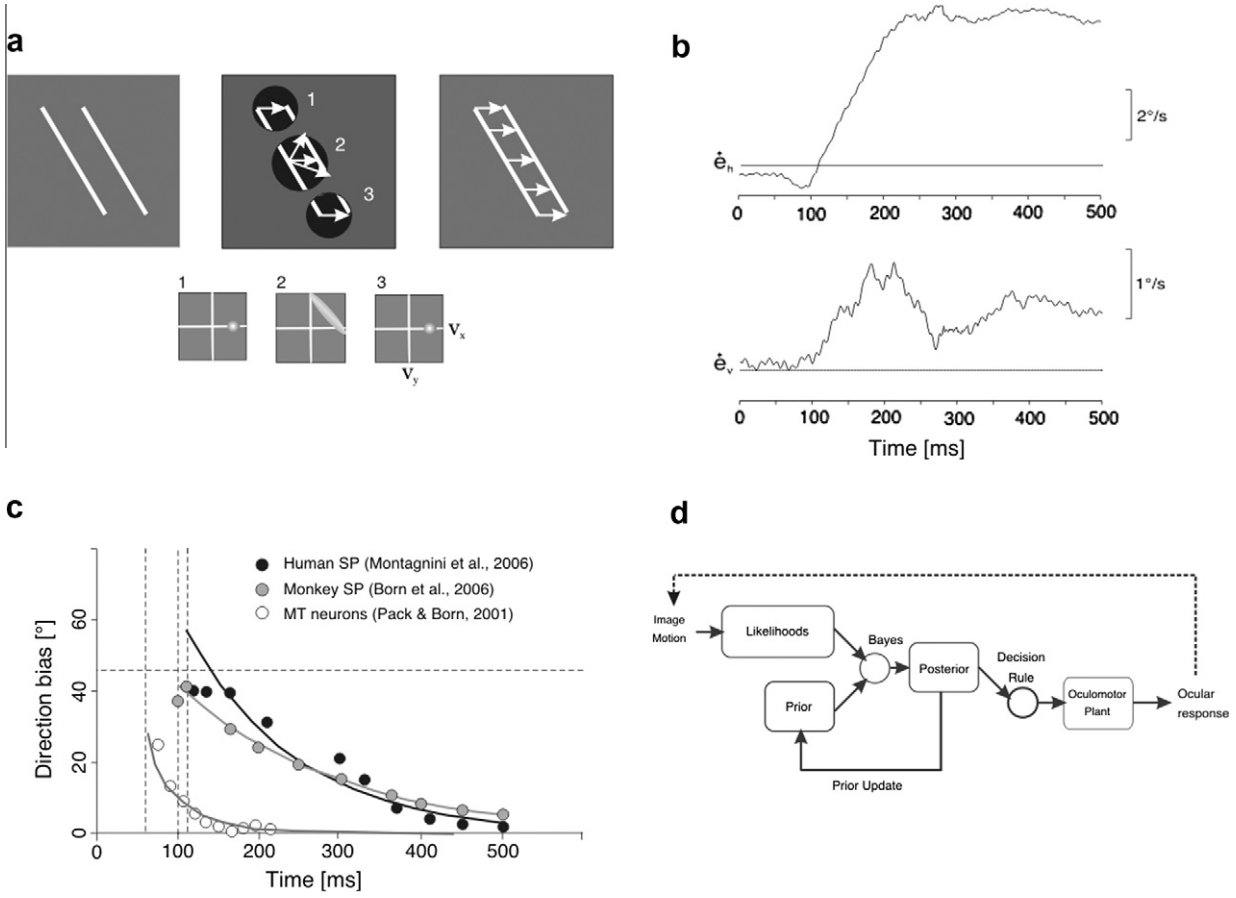

Fig. 1. Aperture problem and dynamics of motion integration. (a) Upper row illustrate the aperture problem during translation of a single tilted line. From left to right: two successive frames of a pure horizontal translation; velocity vectors extracted through three different apertures; the correct solution of the aperture problem is reached when global motion consistent with translation of a rigid object is obtained. Shown are three different instances during pursuit of a tilted line. Lower row illustrates the velocity likelihoods computed at the three locations (ambiguous (2) and unambiguous (1, 3)). (b) Mean smooth pursuit eye velocity traces (horizontal ($\dot{e}_h$) and vertical ($\dot{e}_v$)) for a tilted line translating to right at 7°/s. (c) Pursuit direction error plotted against time for human (black dots) and monkey (gray dots) pursuit of a 45° tilted line. Open circles plot the time course of direction estimate from a population of MT neurons presented with a set of small tilted lines translating in the classical receptive field. (d) Block model of the model for motion inference and pursuit. The front-end infers optimal motion estimation using a Bayesian model. Such estimate is dynamical due to prior updating, implementing a recurrent Bayesian network. The decision rule extracts the optimal image velocity at a given point in time and feeds two independent oculomotor plants, driving horizontal and vertical eye velocity.

visual pattern is recovered has been the goal of dozens of psychophysical and physiological studies (see Bradley & Goyal, 2008; Masson and Ilg (2010) for reviews) but several key aspects remain unclear such as the role of feature motion (Lorenceau & Shiffrar, 1992; Pack, Gartland, & Born, 2004), the rule governing the integration of 1D and 2D local motion (Weiss et al., 2002) or the exact physiological mechanisms used to reconstruct global motion (see Rust, Mante, Simoncelli, & Movshon, 2006; Tlapale, Masson, & Kornprobst, 2010; Tsui, Hunter, Born, & Pack, 2010, for recent computational studies).

A key observation with the aperture problem is that perceived direction of a single tilted bar translating horizontally is biased towards the oblique direction, corresponding to the velocity vector orthogonal to the bar orientation (Castet, Lorenceau, Shiffrar, & Bonnet, 1993; Wallach, 1935), at least for short stimulus durations and low contrast. Such observations also hold for motor actions such as voluntary pursuit. Example of smooth pursuit eye movements driven by a rightward motion of a 45° tilted line is shown in Fig. 1b. At pursuit onset, there is always a transient vertical component, reflecting the directional bias induced by the aperture problem. Once that 2D motion information begins to be integrated along with 1D motion, there is a slow reduction in the directional bias. Such observation was made both in humans (Masson & Stone, 2002; Montagnini, Spering, & Masson, 2006; Wallace, Stone, & Masson, 2005) and monkeys (Born, Pack, Ponce, & Yi, 2006). Fig. 1c plots the time course of the tracking direction error (i.e. the difference between the instantaneous 2D eye movement direction and the 2D translation of the bar) observed in either monkeys (closed symbols) or humans (open symbols). At high contrast, tracking error decays with a time constant ~90 ms so that, after 200 ms of pursuit both eye and target motions almost perfectly matched. Gray symbols plot the time course of the population vector of direction-selective cells recorded from macaque area MT using a somewhat similar stimulus. MT neurons initially respond primarily to the component of motion perpendicular to a contour's orientation, but over a short period of time (time constant: ~60 ms) their responses gradually shift to encode the true stimulus direction 100–150 ms after stimulus onset (Pack & Born, 2001).

Numerous mechanisms such as vector averaging (VA), Intersection of Constraints (IOC) and 2D features (2DFT) (see Bradley & Goyal, 2008, for a review) have been proposed as solutions to the aperture problem. The Bayesian framework, based on the idea that the visual system makes inferences from noisy signals offers a simple explanation for two-dimensional motion illusions observed with a large pool of stimuli (Weiss et al., 2002). Their seminal suggestion was that primate visual system prefers slow and smooth motions. In the Bayesian framework of probabilistic inference, such preference can be instantiated as a Prior distribution centered at

$v_x = v_y = 0$. When presented with 1D motion of single bars, yielding to elongated likelihood distributions, the posterior distribution that is the product of prior and likelihood distributions is centered along the 45° oblique axis, corresponding to the perceived direction along the orthogonal direction. This model was extended to plaid pattern motion direction (Weiss & Adelson, 1998) to demonstrate that it can easily implement the IOC rule by combining different 1D likelihoods. In their model, no specific role was attributed to 2D motion features, thus ignoring some of the information present in the images. However, such framework can be easily extended to combine likelihoods of various local motion cues (1D and 2D) with the slow motion prior into a single path. To account for the different dynamics that are observed for 1D and 2D motion cues respectively (e.g. Masson & Castet, 2002; Masson, Rybarzcyk, Castet, & Mestre, 2000), such two pathways model was proposed, taking into account both the different variances in 1D and 2D likelihoods and their different timing (Barthélemy, Perrinet, Castet, & Masson, 2008).

Although the Bayesian framework gives an accurate account of perception and psychophysical data (e.g. Hurlimann, Kiper, & Carandini, 2002; Stocker & Simoncelli, 2006), this type of models is essentially static. They cannot explain the time course of 2D motion perception as illustrated in Fig. 1c. However, there have been a few attempts to use dynamical inference to solve the aperture problem (e.g. Dimova & Denham, 2010; Montagnini, Mamassian, Perrinet, Castet, & Masson, 2007). A recurrent Bayesian model, where the prior is iteratively updated using the full posterior distribution was proposed by Montagnini et al. (2007) to model such dynamics, using smooth pursuit responses as a hallmark. The variances of the likelihoods and prior in this model were estimated on the basis of an independent set of eye movement data, unlike the other models where these variances were free parameters. In the Bayesian framework, the model output is a posterior distribution that is interpreted as the information used for an optimal perceptual estimate of motion. Different decoding rules can be used such as taking the mean or the maximum a posteriori (MAP) of the distribution, but such value can hardly be compared to the eye movement data. There is thus the need for a realistic oculomotor back end to the Bayesian framework to explain smooth pursuit eye movement data and in particular to render their exact time course. Moreover, our original article stressed the need for additional data in order to better constraint the recurrent model. The present study was conducted to answer these two limitations of the model.

Here, we propose an open loop two-stage model (see Fig. 1d) to explain the dynamics of motion integration in the context of smooth pursuit eye movements. The first step of the model is a sensory information processing stage where likelihoods of all different motion information (as shown in Fig. 1a for different locations) are combined with a prior favoring slow speeds (Weiss et al., 2002). We implemented the different latencies of 1D and 2D likelihoods computation as well as the time constant of the recurrent Bayesian network, assuming that such sensory information stage corresponds to motion processing done in area MT for smooth pursuit (see Lisberger (2010) for a review). The likelihood functions for 1D and 2D and prior are assumed to be Gaussian. The next stage implements the sensorimotor transformation generating the smooth pursuit response as output by taking the maximum a posteriori (MAP) as a decision rule applied to the Bayesian Posterior and using it as input. For simplicity, we model the dynamics of motion integration in an open-loop phase mode, ignoring the oculomotor feedback (dotted line). A main objective of the study was to determine the model parameters from a set of "pure" 1D and 2D stimuli and test it against a full set of tilted bars, presented at different contrast and speed values. In addition, our implementation of the oculomotor plant attempts to take into account the directional anisotropies affecting smooth pursuit as well as the possible non-linearities due to the use of extended line drawings instead of the classical moving dots. Our two-stage model could reproduce in considerable detail the individual mean eye velocity traces for subjects tracking tilted lines. In particular, we could mimic the transient directional bias due to the aperture problem and the dynamic motion integration as its solution as well as its sensitivity to different low-level image attributes.

2. Methods

2.1. Experimental methods

To estimate both likelihood and prior variances for the recurrent Bayesian model, as well as to tune the parameters of the oculomotor plant, we performed a new set of experiments. Eye movements were recorded from two observers, both authors (AM and GM) and naïve subjects (JD (*experiment 2*) & AR (*experiment 3 – varying contrast*)) using the ReX software package running on a PC with the QNX Momentics operating system. The ReX PC controlled both stimulus presentation and data acquisition (see details in Masson, Rybarzcyk, Castet, & Mestre, 2000). Stimuli were generated with an Sgi Octane workstation and back-projected along with the red fixation point onto a large translucent screen ($80 \times 60°$) using a 3 CRT video-projector (1280×1024 pixels at 76 Hz). The peak luminance of the stimuli for all experiments was of 45 cd/m^2. We have divided the conditions into: (i) a contrast set, with stimuli moving at a steady velocity of 7°/s for three different contrast conditions (10%, 30% and 90%) against a gray background and (ii) a velocity set, described as stimulus moving at 100% contrast for three different speeds (5°/s, 10°/s and 15°/s) against a dark background.

For all experiments, observers had their head stabilized by chin and forehead rests. Each trial started with the presentation of a fixation point for a random duration of 600 ± 100 ms. Observers were required to fixate within a $1° \times 1°$ window. The fixation point was then extinguished and the motion stimulus was presented after a 350 ms blank. The object moved for 500 ms. Observers were instructed to track the object center and trials were aborted if eye position did not remain within a square window of 5° width, located at the object center. All conditions were randomly interleaved to minimize cognitive expectations and anticipatory pursuit. We collected a minimum of 80 and a maximum of 100 trials per condition for each observer over several days.

Vertical and horizontal position of the right eye was recorded at a sampling rate of 1 kHz by means of the scleral eye coil technique and low-pass filtered (Collewijn, van der Mark, & Jansen, 1975). Eye-position data were linearized, smoothed with a spline interpolation (Busettini, Miles, & Schwarz, 1991) and then differentiated to obtain vertical and horizontal eye-velocity profiles. After visual inspection using MATLAB, we used a conjoint velocity and acceleration threshold to detect and remove saccades (Krauzlis & Miles, 1996). Latency of each trial was computed for both horizontal and vertical eye-velocity profiles using an objective method (Krauzlis & Miles, 1996; Masson & Castet, 2002). Oculomotor traces were aligned to the stimulus onset. An offline inspection was done to eliminate outlier trials (less than 5%). The outlier trials are those in which saccades could not be eliminated without excluding the majority of the trial or in which high levels of noise exist during fixation and persist during pursuit.

2.2. Experiment 1: pursuing pure 1D and pure 2D stimuli

In order to estimate the initial prior and likelihood variances of the Bayesian inference from the smooth pursuit responses of pure 1D and pure 2D stimuli, subjects were asked to pursue "pure 1D"

(48° long line) and "pure 2D" (blob) stimulus. The "pure 2D" stimulus is a central blob with Gaussian luminosity profile (standard deviation ~0.2° of visual angle). The 48° long vertical has terminators far in the peripheral visual field and thus their influence was assumed to be limited. Therefore this stimulus can be approximated to a "pure 1D" stimulus. The target was moving horizontally to the right or left, for both contrast and velocity sets of conditions.

2.3. Experiment 2: effect of line length on smooth pursuit

We investigated the effect of line length on different properties of smooth pursuit. Latency and eye velocity during either initial acceleration or steady-state time windows provide an account of the oculomotor dynamics in the smooth pursuit response. Keeping the edge motion direction and orientation constant, we varied line length to tune the oculomotor gain parameters in the model. The stimuli were a blob (control condition) and vertical lines of lengths 5°, 10°, 20° and 48° moving horizontally rightward or leftward, with three different contrast values.

2.4. Experiment 3: directional anisotropies in initial and steady-state velocities

To define horizontal and vertical oculomotor plants of the model, we needed to evaluate any directional anisotropies and consider them while tuning plant parameters. This is particularly important for a model where several parameters are estimated from the variance of the motor responses. To do so, we used a line of length of 17°, moving orthogonal to its orientation in four cardinal and four diagonal directions. These eight motion directions were presented interleaved, at three contrast (10%, 30% and 90%, fixed speed: 7°/s) values and three speeds (5, 10 and 15°/s, 100% contrast).

2.5. Experiment 4: pursuing a tilted line

We compared the model eye velocity traces with human smooth pursuit responses obtained with a tilted line for which initial perceived direction is biased towards the orthogonal axis. Subjects were instructed to track a 45° tilted line (length: 17°) translating horizontally, either rightward or leftward. Such 45° tilted line was presented at three different speeds (5, 10 and 15°/s) and contrast (10%, 30% and 90%). All conditions were presented interleaved.

2.6. Mathematical methods: tuning the Bayesian recurrent model

The variances of the likelihood functions were estimated from smooth pursuit data. Assuming that variance in smooth pursuit response almost entirely comes from the sensory source (Osborne, Lisberger, & Bialek, 2005), the variance of the smooth pursuit responses to a reference stimulus (i.e. either "pure 1D" or "pure 2D") was considered as the posterior variance and used to estimate respective likelihood variance and prior variance. The prior was assumed to favoring slow speeds. This estimation of likelihood variance was done for different speeds since we know that speed is not homogeneously represented in MT (DeAngelis & Uka, 2003) as well as for different contrasts since their parameters are known to influence both perceived direction (Lorenceau, Shiffrar, Wells, & Castet, 1993) and pursuit initiation (Spering, Kerzel, Braun, Hawken, & Gegenfurtner, 2005) . We used the mean eye velocity measured in a 40 ms time interval centered at the peak acceleration time as an approximate estimate of the posterior distribution variance considering that the open loop dynamics might better reflect the initial posterior function (Montagnini et al., 2007).

As noted in the introduction, the visual stimulus has 1D (edge related) and 2D (terminator related) motion information. We assume both of them to be independent and Gaussian distributions. If v_0 is velocity of the stimulus, the likelihood function L_1 for the edge-related information (1D) in velocity space (v_x, v_y) is given by

$$L_1 = \frac{1}{Z}\exp\left(-\frac{((v_x - v_0)\cos\theta + v_y \sin\theta)^2}{2\sigma_1^2}\right) \quad \text{(See Fig. 6)} \tag{1}$$

where Z is the partition function (used in this section, for all distributions), θ is the orientation of the line relative to the vertical, taken as positive in anti-clockwise direction and σ_1 is the standard deviation of the speed in the orthogonal direction to the line. The likelihood function L_2 for the terminator-related information in velocity space (v_x, v_y) is given by

$$L_2 = \frac{1}{Z}\exp\left(-\frac{(v_x - v_0)^2 + v_y^2}{2\sigma_2^2}\right) \tag{2}$$

where σ_2 is the standard deviation of the speed. The overall likelihood function is the product of the two likelihoods 1D and 2D (since, both are assumed to be independent):

$$L(v_x, v_y) = L_1(v_x, v_y)L_2(v_x, v_y) \tag{3}$$

Assuming a prior favoring slow speeds (mean centered at origin) and directionally unbiased (normally distributed with a variance σ_0), the initial prior P_0 can be written in velocity space (v_x, v_y) as

$$P_0 = \frac{1}{Z}\exp\left(-\frac{v_x^2 + v_y^2}{2\sigma_0^2}\right) \tag{4}$$

The likelihood function (L) is combined with the initial prior (P_0) using bayes rule to obtain the initial posterior distribution (Q_0)

$$Q_0(v_x, v_y) = L(v_x, v_y)P_0(v_x, v_y) \tag{5}$$

To obtain a read out of the distribution that is used for the later stages a decision rule called maximum-a posteriori (MAP), in this case equivalent to the mean of the distribution is implemented as:

$$(\widehat{v_x}, \widehat{v_y}) = argmax(v_x, v_y)Q_0(v_x, v_y) \tag{6}$$

The posterior distribution at every instant t is used to dynamically update the prior (recurrent Bayesian framework) that is used for the next iteration which is expressed as:

$$P_t(v_x, v_y) = Q_{t-1}(v_x, v_y) \tag{7}$$

This recurrent Bayesian framework can be summarized as:

$$Q_t(v_x, v_y) = L(v_x, v_y)P_t(v_x, v_y) \tag{8}$$

The variance terms σ_0^2, σ_1^2 and σ_2^2 are estimated applying Bayes rule to pure 1D and pure 2D motion stimuli (experiment 1):

$$Q_{0,i}(v_x, v_y) = L_i(v_x, v_y)P_0(v_x, v_y) \tag{9}$$

with $i = 1$ and 2 for 1D and 2D stimulus respectively. Given that both the likelihoods and prior are normal distributions, their product is also a normal distribution. Thus it is possible to write two simple equations relating the means and variances of the three distributions involved in Eq. (9), yielding:

$$\begin{cases} \mu_{Q_{0,i}}\sigma_{Q_{0,i}}^{-2} = \mu_i\sigma_i^{-2} + \mu_0\sigma_0^{-2} \\ \sigma_{Q_{0,i}}^{-2} = \sigma_i^{-2} + \sigma_0^{-2} \end{cases} \tag{10}$$

The values $\mu Q_{0,i}$ and $\sigma_{Q_{0,i}}^{-2}$ are estimated from the oculomotor recordings for the 1D and 2D stimulus respectively. The likelihood mean value μ_i assumed to be stimulus speed v_0 and prior mean μ_0 is assumed to be zero, initially. The above set of equations provide us with two values for the variance of prior one each for $i = 1$ and $i = 2$ conditions. The final prior variance is taken as the average of the two.

The evolution of the posterior across time is evaluated numerically, by means of an iterative algorithm. However, note that analytical derivations are possible given the assumption of normal distribution (see Montagnini et al., 2007).

3. Results

3.1. Experiment 1: tuning the recurrent Bayesian model with variances of pursuit responses to a blob or a line of varying contrast

To estimate the prior and likelihood variances of the Bayesian inference from the smooth pursuit responses to pure 1D and pure 2D stimuli, subjects were asked to pursue 1D (48° long vertical line) and 2D (blob) stimulus. In Fig. 2, mean velocity profiles of pursuit responses to either a "pure" 2D (Fig. 2a) or a "pure" 1D stimulus (Fig. 2b) of three different contrasts are shown for subject GM. The shaded area around the smooth pursuit traces represents the standard deviation across all trials for all times during the pursuit. Standard deviation of mean eye velocity computed in the peak acceleration time window (shown in Fig 2a and b) is plotted against contrast for the two subjects and each stimulus type in Fig. 2C. Overall, variance of pursuit responses decreased with higher contrast values. In particular, with the "pure 2D" stimulus standard deviation of responses in the peak acceleration time window regularly decreased with increasing contrast. With upright moving lines, at very low contrast, we found a decrease in eye velocity variance, which could be related to a large reduction in initial eye velocity. A stronger variance was observed at 30% contrast for both the subjects. The variance of the pursuit response in the peak acceleration time is used to estimate the prior and likelihood variances as described in the mathematical methods. The latency for 1D stimulus for three contrasts spans in the interval 90–110 ms, which is lower compared to the latency for 2D stimulus (110–160 ms). For both stimuli, we found a decrease in latency with an increase in the contrast of the stimuli. The mean response to the 2D stimulus is much slower compared to the 1D stimulus, accounting for the difference in the energy of the stimuli.

3.2. Experiment 2: using effects of line length to tune the 2D oculomotor plant

Next, we considered the effect of line length while tuning the parameters of the oculomotor plant. We recorded smooth pursuit responses to stimuli consisting of blob, and vertical line of varying lengths (5°, 10°, 20°, 48°). The blob is considered to be a limiting case and is excluded from the statistical repeated measures 2-way ANOVA test. Fig. 3a plots mean eye-velocity profiles for blob motion (black curve) and lines of increasing lengths. Fig. 3b–d illustrates the changes in different parameters. Latency exhibited a consistent dependence upon line length, in particular at low

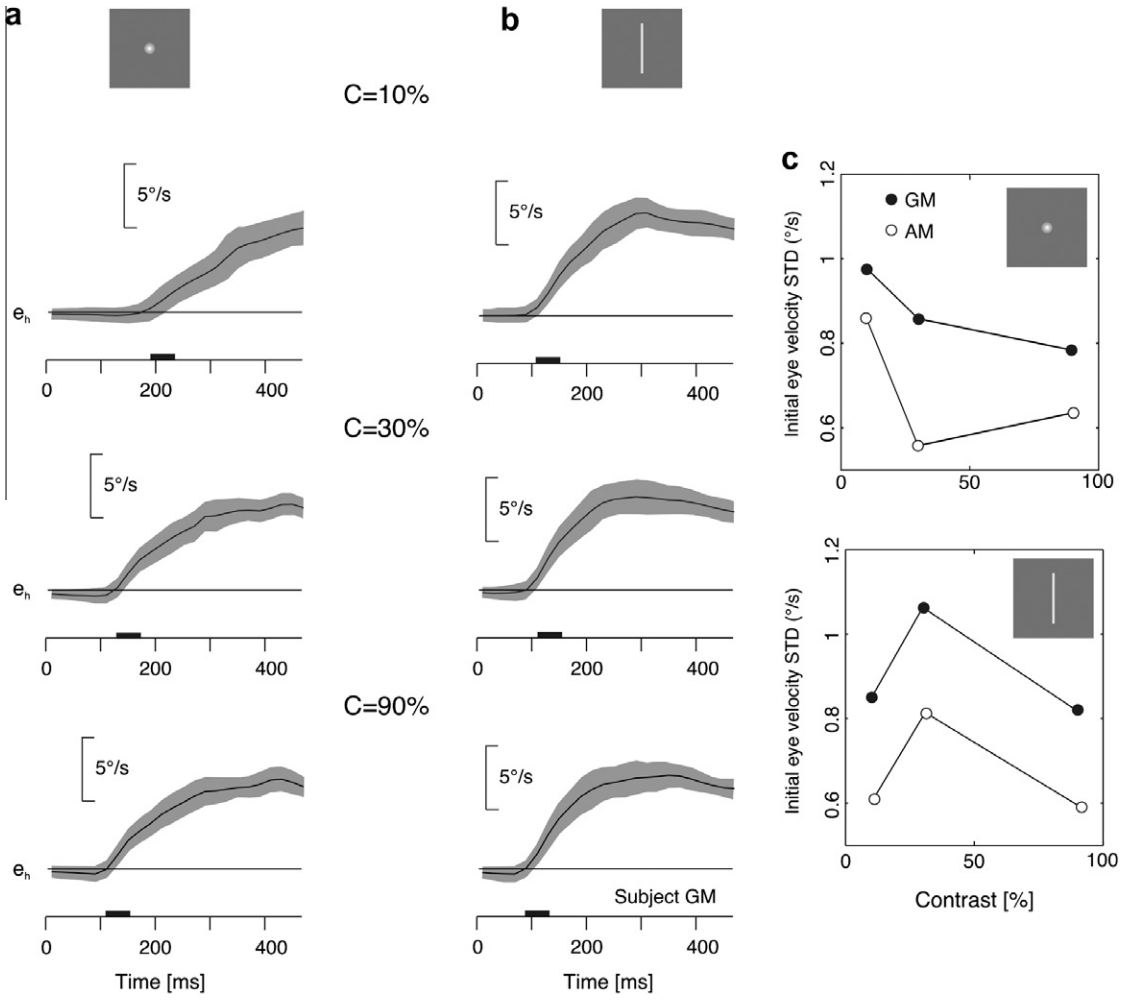

Fig. 2. Pursuing pure 1D and pure 2D stimulus. Mean eye-velocity profiles of pursuit responses to a blob (a) or a 48° long line (b), presented at three different contrasts. Profiles of standard deviation of eye velocity (across trials) is illustrated by the gray shaded area. The bars shown on the time axes indicate the peak acceleration time window(c) Standard deviation in the peak acceleration time window is plotted against contrast, for the two objects and two subjects.

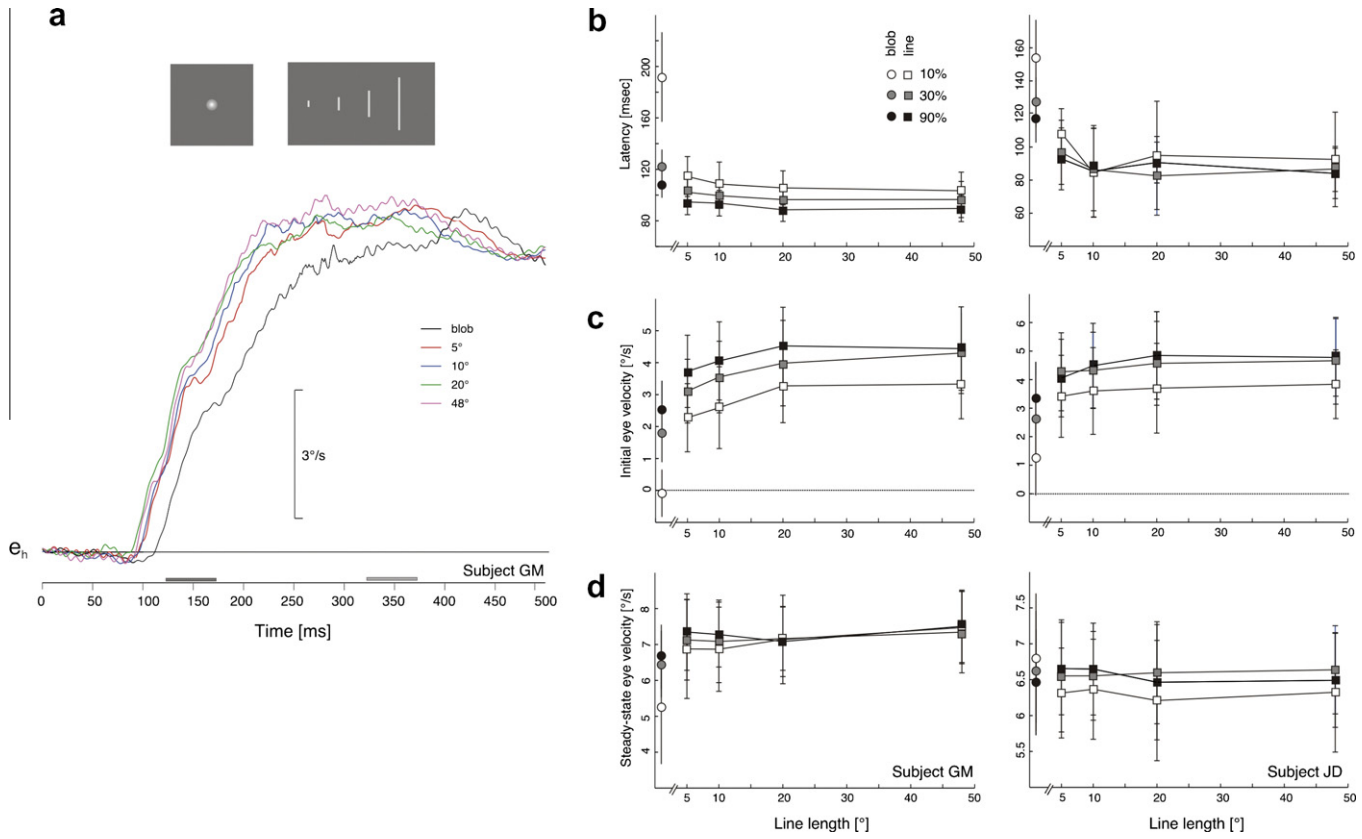

Fig. 3. Effect of line length. (a) Mean eye-velocity profiles of pursuit responses to either blob or lines of different lengths. (b) Mean latency of horizontal pursuit for blobs (circles) and lines (squares), plotted against line length. (c and d) Dependency of initial and steady-state eye velocity upon line length, for three different contrasts. Subject GM. Similar data were obtained with Subject AM.

contrast. The statistical repeated measures 2-way ANOVA test done indicated a significant effect of contrast ($F(2, 1015) = 154.4$; $p < 0.0001$) and line length ($F(3, 1014) = 19.92$; $p < 0.0001$). There is no interaction between the two factors ($F(6, 1006) = 1.22$ and $p < 0.2923$). For any given line length, higher contrast resulted in shorter latency. The mean latency difference between blob and line conditions was of ~75 ms for a length of 5° and a contrast of 10% and was reduced to less than 20 ms by increasing contrast to 30% and 90%. At high contrast (30% and 90%), line lengths above 20° affected only little pursuit latency. There was a small decay to pursuit latency with line length in the range 5–20°. This seems to indicate to a fast decaying type of dependence of latency on the amount of 1D information in the stimulus.

The mean of the initial pursuit velocity in the [120, 180 ms] time window is plotted for different contrast conditions against line length in Fig. 3c. The ANOVA test indicated a significant effect of contrast ($F(2, 1015) = 113.63$; $p < 0.0001$) and line length ($F(3, 1014) = 41.12$; $p < 0.0001$) upon initial eye velocity. There is no interaction between the two factors ($F(6, 1006) = 0.9$; $p < 0.4946$). The relationship between initial eye velocity and line length was inverted when compared to the modulation found for latency. Across all line lengths, higher contrast resulted in higher eye acceleration. The difference between mean velocities for blob and 5° long line at 90% contrast was of ~1.2°/s and increased gradually when lowering contrast, from 1.32°/s at 30% contrast to 2.3°/s at 10% contrast. Initial eye velocity increased with longer lines in the range 5–20° and then saturated with longer bars, irrespective of contrast.

Lastly, we analyzed steady-state tracking by measuring eye velocity in the [320, 380 ms] time window. Steady-state eye velocity (mean ± SD across trials) is plotted against line length, for the three different contrast values in Fig. 3d. The ANOVA conducted on steady-state eye velocity showed significant effect of line length ($F(3, 1014) = 7.73$; $p < 0.0001$) and an effect of contrast ($F(2, 1015) = 4.86$; $p < 0.0079$) at least for smaller line lengths (=<10°) and a non-significant interaction between the two parameters ($F(6, 1006) = 1.87$; $p < 0.0823$). For line lengths 5° and 10°, higher the contrast, higher is the velocity in the steady-state. The difference between the velocities of blob to that of 5° long line at 10% contrast (1.6°/s) decreases to (0.7°/s) at 90%. With increasing line length above 10°, the differences in the steady-state velocity for different contrasts cease to exist.

These results clearly indicate an effect of line length at least for line lengths less than 20° on latency, velocities in peak acceleration time window for any given contrast. This effect is coherent with the size of spatial integration for human pursuit (Heinen & Watamaniuk, 1998). These results indicate that we need to consider low-level properties of the moving target such as line length and contrast when tuning parameters of the oculomotor model.

3.3. Experiment 3: using directional anisotropies to tune a 2D oculomotor model

We recorded pursuit responses to a single line of length (17°) moving in different directions in order to probe directional anisotropies to be considered when tuning an oculomotor model for simulating two-dimensional pursuit responses as those obtained with tilted lines (see Fig. 1). In the third experiment, we presented a line (length: 17°) moving orthogonal to its orientation along four cardinal and four diagonal directions. We collected data at different speeds (5, 10 and 15°/s, fixed contrast: 100%) and contrasts (10%, 30% and 90%, fixed speed: 5°/s).

Horizontal ($\dot{e}_h$) and vertical ($\dot{e}_v$) components of smooth pursuit responses to a line moving along the directions in the first quadrant (0°, 45° and 90°) at two different speeds are shown in Fig. 4a. Clearly, responses to motion along different directions exhibited different dynamics, which were scaled with target speed. For each motion direction, we measured latency, initial and steady-state eye velocities of both horizontal and vertical components of two-dimensional pursuit. The horizontal and vertical component latencies of the responses along all eight directions for different speeds are shown in Fig. 4b. We observed differences between h-latency and v-latency for target motion along diagonal directions that were highly idiosyncratic, as reported by Soechting, Mrotek, and Flanders (2005). The mean initial velocity computed in the early time window [120, 180 ms] is shown in Fig. 4c. An ANOVA test revealed a significant main effect of motion direction (Subject GM: $F(7, 1888) = 23.21$; $p < 0.0001$; Subject AM: $F(7, 1769) = 55.88$; $p < 0.0001$), indicating that some directions yielded stronger eye accelerations. However, the characteristics of directional anisotropies were again highly idiosyncratic. Main effect of speed indicated that higher speeds resulted in stronger eye accelerations (Subject GM: $F(2, 1893) = 42.48$; $p < 0.0001$; Subject AM: $F(2, 1774) = 41.61$; $p < 0.0001$). We found significant interactions between direction and speed (Subject GM: $F(14, 1872) = 2.06$; $p < 0.01$; Subject AM: $F(14, 1753) = 8.87$; $p < 0.0001$), indicating that anisotropies changed with target speed. The mean steady-state eye velocity was measured over the [320, 380 ms] time window and is plotted in Fig. 4d. Again, there was a significant effect of target motion direction (Subject GM: $F(7, 1888) = 32.34$; $p < 0.0001$; Subject AM: $F(7, 1769) = 89.04$; $p < 0.0001$), indicating that pursuit had higher gain for some directions. Interestingly, for both subjects, such directional anisotropy disappeared at very low speed. The interactions between direction and speed were significant. (Subject GM: $F(14, 1872) = 17.31$; $p < 0.0001$; Subject AM: $F(14, 1753) = 39.59$; $p < 0.0001$), again indicating that anisotropies in measured eye velocity are speed-dependent.

We performed a similar analysis for smooth pursuit responses to different motion directions, presented at three different contrasts. Fig. 5a plots both horizontal (continuous lines) and vertical (broken lines) latency, for eight motion directions and three contrasts, for subjects GM (first column), AM (second column) and AR (third column). Consistent with the previous experiment, both horizontal and vertical latencies were shorter across all directions for higher contrast values. Again, there are subject-specific differences between x-latency and y-latency for some diagonal directions (Soechting et al., 2005).

The mean initial eye velocity in the time window (120, 180 ms) is shown in Fig. 5b. There are clearly some subject-specific anisotropies, indicating stronger eye acceleration for some motion directions than for others. An ANOVA revealed a significant main effect of motion direction (Subject GM:

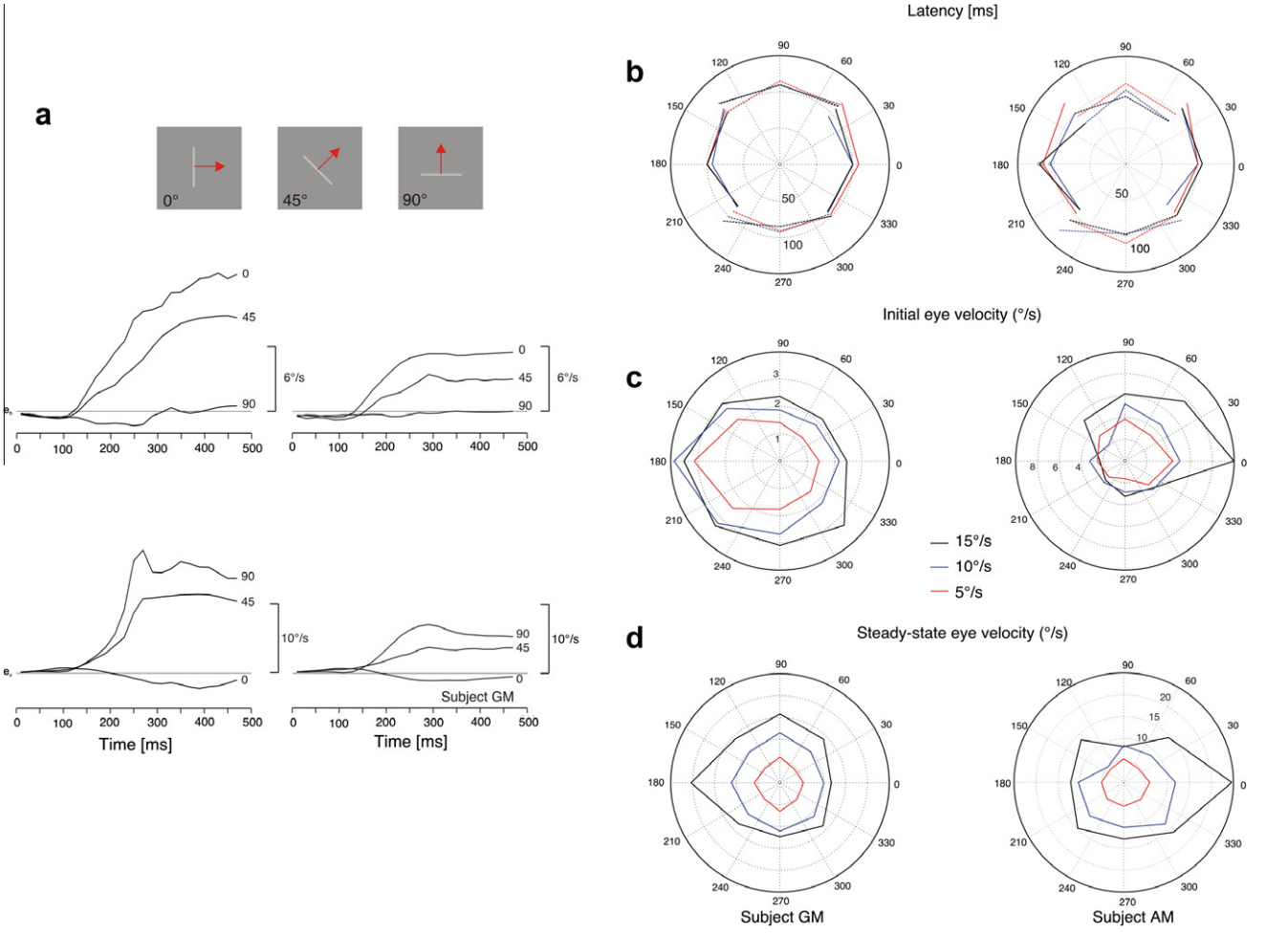

Fig. 4. Directional anisotropies of speed. (a) Mean velocity profiles of pursuit responses to a 17° long line, moving orthogonally to its orientation along three directions (0°, 45° and 90° shown at the top of the figure with red arrows), for two different speeds (left panel: 15°/s, right panel: 5°/s (horizontal component ($\dot{e}_h$) – top; vertical component ($\dot{e}_v$) – bottom)). (b) Mean horizontal (shown by solid line) and vertical (shown by dotted line) latencies, for all eight motion directions and 3 speeds. (c and d) Directional anisotropies for initial and steady-state eye velocity, respectively. Colors indicate different target velocities. Left and right panels are for subject GM and AM, respectively.

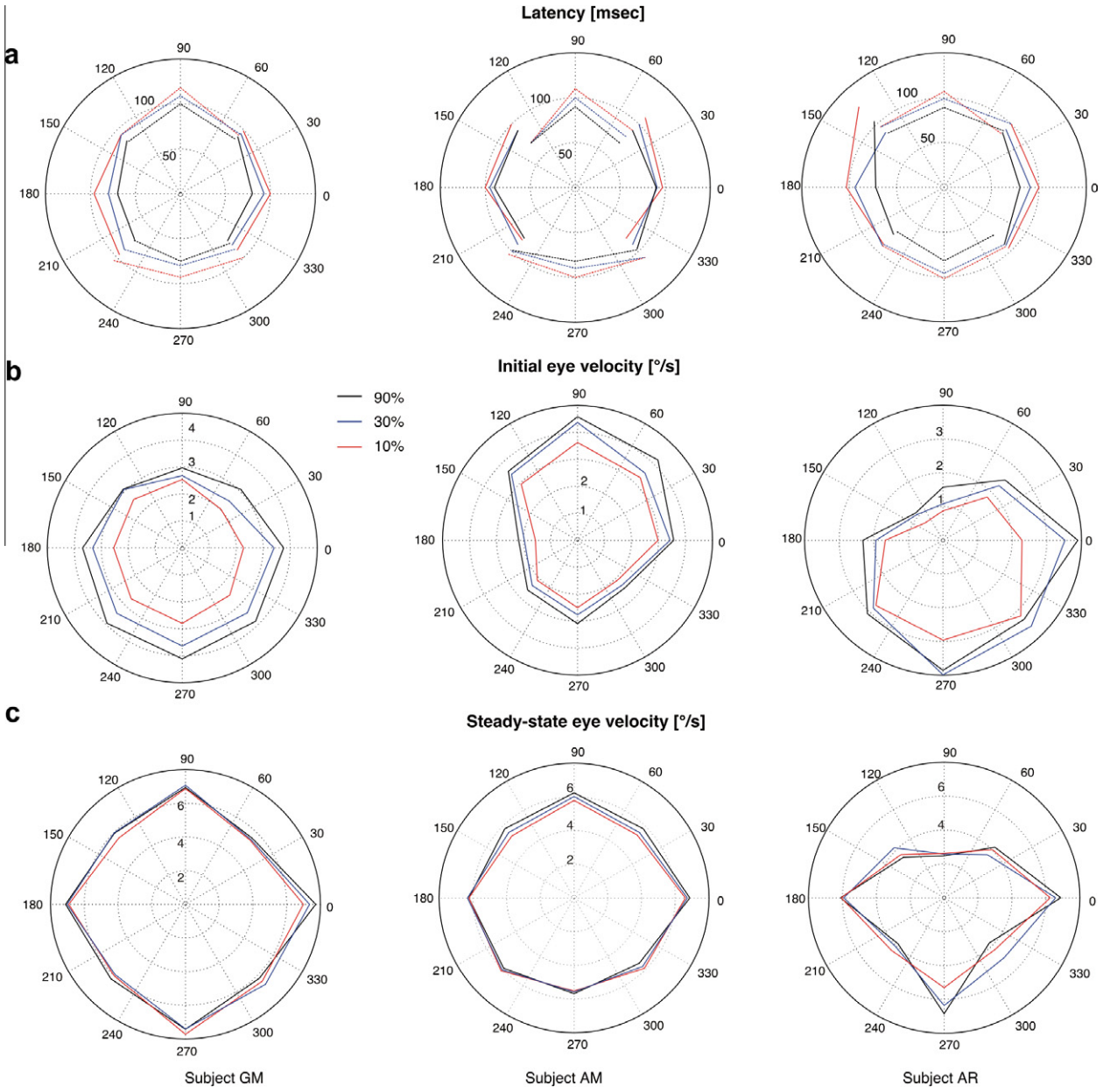

Fig. 5. Directional anisotropies of contrast. Directional anisotropies for pursuit latencies (a), initial eye velocity (b) and steady-state eye velocity (c), for three different target contrasts. Three columns are for subject GM, AM and AR respectively.

$F(7, 1887) = 17.38$; $p < 0.0001$; Subject AM: $F(7, 2137) = 177.35$; $p < 0.0001$; Subject AR: $F(7960) = 49.05$; $p < 0.0001$) and, again, of contrast (Subject GM: $F(2, 1892) = 88.66$; $p < 0.0001$; Subject AM: $F(2, 2142) = 40.08$; $p < 0.0001$; Subject AR: $F(2965) = 16.46$; $p < 0.0001$). The main direction effect indicates that initial eye velocity is strongly directionally anisotropic and idiosyncratic. For example, the initial eye velocity (subject: AM) along 180° is 1.6°/s which is significantly lower when compared to the initial eye velocity (3.63°/s) reached at the same point in time when pursuing in the upward direction (90°). On the contrary, the effect of contrast was directionally isotropic: across all motion directions, initial eye velocity increased with contrast. For the three subjects, varying contrast did not change the idiosyncratic directional anisotropies. Similar results were observed with steady-state eye velocity, as computed in the [320–380 ms] time window (Fig. 5c). A main effect of direction was found when performing an ANOVA test (Subject GM: $F(7, 1887) = 77.06$; $p < 0.0001$; Subject AM: $F(7, 2137) = 56.91$; $p < 0.0001$; Subject AR: $F(7960) = 27.2$; $p < 0.0001$). Interestingly, the main directions for steady-state eye velocity were different from those observed with initial eye velocity. Again, contrast only marginally modulated steady-state eye velocity (Subject GM: $F(2, 1892) = 4.68$; $p < 0.009$; Subject AM: $F(2, 2142) = 8.24$; $p < 0.0003$) and the interaction between direction and contrast factors was marginally significant (Subject GM: $F(14, 1871) = 1.99$; $p < 0.01$; Subject AM: $F(14, 2121) = 2.99$; $p < 0.0001$). However, one can notice that steady-state eye velocity was almost identical across all eight motion directions with very low contrast (red curves). These results suggest that subject specific directional anisotropies indeed exist for different conditions (Tanaka & Lisberger, 2001) and should be taken into consideration when tuning the parameters of the oculomotor plant.

3.4. A recurrent Bayesian model for dynamic motion integration

We propose a recursive extension to the Bayesian framework (Weiss et al., 2002) to describe the dynamic integration of 1D and 2D motion information. In the recurrent Bayesian framework (Montagnini et al., 2007), the prior defined in the velocity space is combined with the two independent measurement likelihood functions (likelihood functions representing edge-related (1D) and terminator-related information (2D)) to obtain the posterior, which updates the prior at the end of the iteration.

3.5. Model description

The block diagram of the model is illustrated in Fig. 6. The model consists of three blocks, from left to right. The first block describes the sensory information processing as a recurrent Bayesian network and incorporates some fixed delays. The output is read out using Maximum-A-Posteriori (MAP) rule to extract desired horizontal and vertical eye velocity. These dynamical signals are then converted into eye velocity by two independent oculomotor plants.

The 1D and 2D motion information likelihoods are delayed by δt_{1d}, a fixed sensory delay of 20 ms. In addition to that, the 2D information is delayed (δt_{2d}) by a fixed lag of 50 ms. This lag results in (50–70 ms) time delay for the initiation of encoding the true global velocity of the stimulus which is in agreement with the dynamics of motion signaling by neurons in MT (Smith, Majaj, & Movshon, 2005). The consequence of this delay is that 1D information is dominant in the initial stages of motion integration. It was long enough to allow a sufficient response from the filter implementing the oculomotor plant. The prior is updated with the posterior at the end of each iteration step with a delay (δt_{fb}). This delay accounts for the transient in the MAP of the recurrent Bayesian network. The horizontal and vertical MAP transient is also shown in Fig. 6 as inputs to the respective oculomotor plants. The time constant of the vertical component of the Bayesian MAP is fixed around 65 ms with δt_{fb}, in agreement with the time constant of the change in preferred direction as observed with a population of MT neurons (Pack & Born, 2001; see Fig. 1c).

The recurrent Bayesian network is cascaded with a Proportional-Derivative (PD) control model (Goldreich, Krauzlis, & Lisberger, 1992) to mimic the oculomotor dynamics and produce

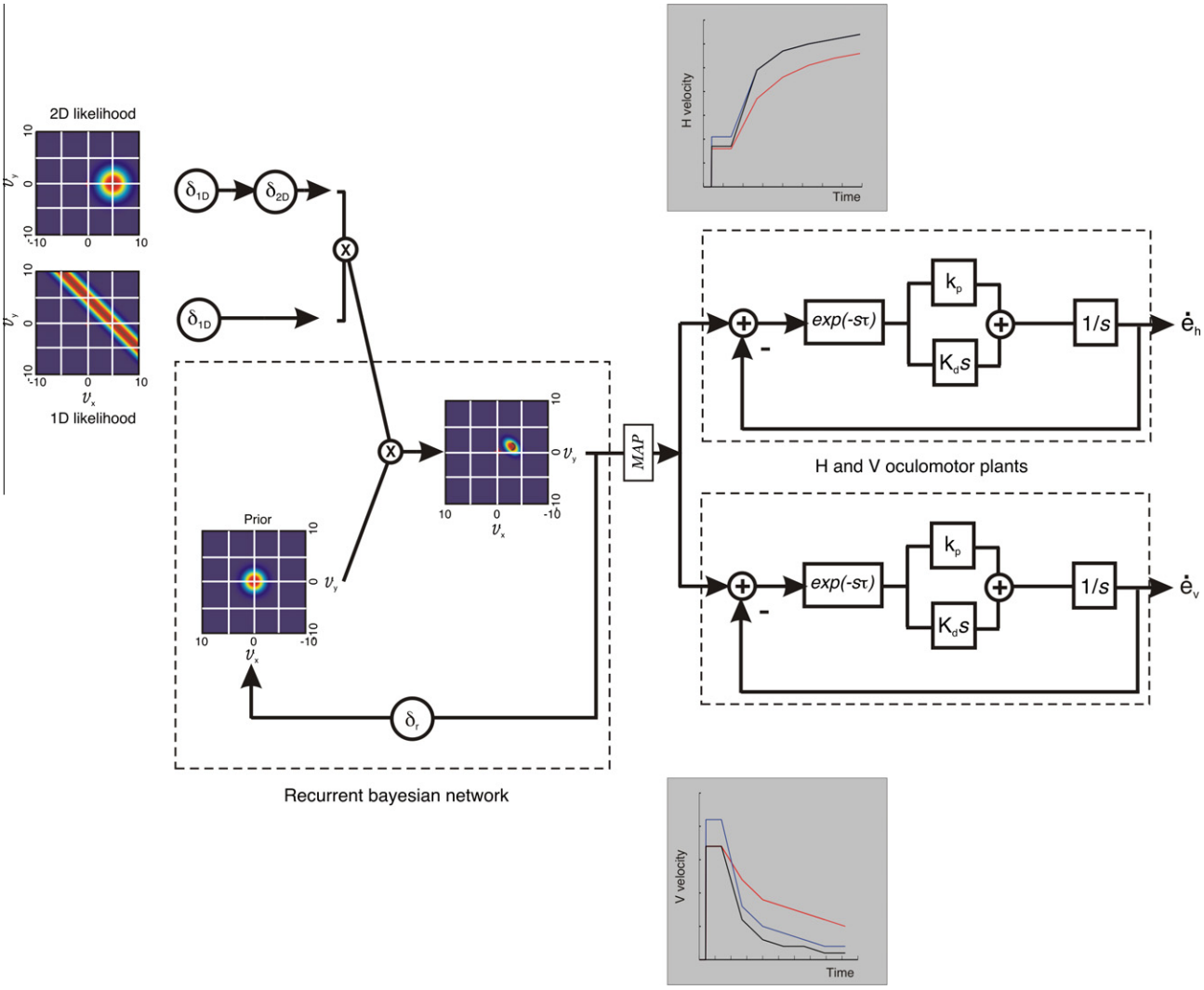

Fig. 6. Model of recurrent inference for pursuit eye movements. The 1D and 2D motion information likelihoods are delayed by δ_{1D} and $(\delta_{1D} + \delta_{1D})$ respectively, and combined with the prior in a recurrent Bayesian framework. The prior is updated by the posterior for every δ_{fb} ms. The readout of the posterior is obtained using the maximum-a posteriori (MAP) decision rule. The transient of the horizontal and vertical components of the MAP (shown at the top and bottom in gray plots respectively for three different contrasts 10 % (red), 30 % (blue) and 90 % (black)) are fed as inputs to the horizontal (H) and vertical (V) oculomotor plants to produce pursuit velocity traces $\dot{e}_h$ and $\dot{e}_v$ respectively.

velocity traces comparable to the smooth pursuit eye velocity traces. The PD control essentially is a first order control system consisting of a delay τ, along with a proportional gain k_p and derivative gain k_d. The proportional gain k_p is directly proportional to the speed error signal whereas the differential gain k_d is proportional to the change in error. The latency of pursuit onset for the model is the sum of the fixed sensory delay δt_{1d} and the variable oculomotor delay τ.

3.6. Tuning the model parameters

Since the timing parameters in the recurrent Bayesian model are fixed delays, the parameters that remained to be tuned were k_d, k_p, τ. The delay τ is a free parameter and its value is equal to the latency of pursuit onset as measured in the above mentioned experiments. Knowing both the effects of line length (Fig. 3) and directional anisotropy (Figs. 4 and 5), we choose to tune the horizontal and vertical oculomotor plant gain parameters across all conditions (different speeds and different contrasts) with the smooth pursuit horizontal and vertical components respectively for a line of same length as the tilted line and moving orthogonal to its orientation along the 45° diagonal since the initial dynamics of the smooth pursuit response for a 45° tilted line is biased toward the 45° direction because of the aperture problem. The fixed delay values in the recurrent Bayesian block for the two subjects are shown in the Table 1. The parameters of horizontal and vertical oculomotor plants obtained for both the subjects (AM and GM) across the different conditions are shown in Table 2. The parameters are estimated using a least square error fit.

3.7. Experiment 4: model and Smooth pursuit responses to translating tilted lines

We compared human pursuit and model using a different set of stimuli, tilted lines, where the aperture problem results in different initial and steady-state perceived directions, as show in Fig. 1. The velocity traces of the model and smooth pursuit responses obtained with such as 45° tilted line are presented for three different contrast values in Fig. 7. After pursuit onset, there was a transient vertical component observed for both model and the data, reflecting the directional bias in the initial pursuit direction as previously observed (Masson & Stone, 2002; Born et al., 2006; Montagnini et al., 2006). Such bias corresponds to the shift in perceived direction due to the aperture problem. As expected, lower contrast resulted in stronger vertical eye acceleration and thus stronger pursuit bias towards the direction orthogonal to the bar orientation. Once the 2D motion information was integrated into target motion estimation, a rapid reduction in the vertical response component was observed, corresponding to a gradual rotation of pursuit direction towards the true translation direction. In the recording time window, such steady-state bias was remarkably reduced when target contrast increased. The model reproduced all of these observations. In particular, lower contrast resulted in delayed pursuit onset and stronger vertical responses. Interestingly, even for higher contrasts the steady-state vertical bias didn't cancel out over the time scale under investigation. The steady-state vertical bias for the model completely disappeared at high contrast for much longer pursuit duration (~1000 ms). The horizontal component of the model response was slower as compared to that in data, particularly during the initial 50 ms (20–70 ms of MAP dynamics in Fig. 6) where the model responded to 1D information alone, delaying the steady-state phase. Lastly, steady-state eye velocity (horizontal component) of smooth pursuit responses increased with contrast, in agreement with Spering et al. (2005). Root mean square deviation (RMSD) values for the model and mean smooth pursuit traces for a moving tilted line are shown in Table 3. Since the model is for the open loop, we have evaluated RMSD for duration of 250 ms, starting from 20 ms before pursuit initiation to 230 ms after pursuit initiation. The RMSD values indicate that the model provides a quantitative description of the motion integration which is close to what is observed in smooth pursuit data, especially in the open loop.

The horizontal and vertical components of the model responses for different speeds are shown in Fig. 8, in comparison with human pursuit. At pursuit onset, a transient vertical component was observed for all speeds. Maximum velocity of such transient vertical component increased with target speed, for both human data and model, as found by Wallace et al. (2005). A slow reduction in the vertical component leads to a steady-state bias, which again scaled with target velocity. Model output resulted in a gradual increase in both horizontal and vertical eye velocity with increasing target speed, indicating that inference is further biased at high speed. The steady-state velocity (horizontal component) of the smooth pursuit response was accurate for lower speeds but overestimated target speed, in particular for higher speed (15°/s).

The dynamics of the direction bias is better illustrated when plotting initial tracking error against time (Fig. 9) for both the smooth pursuit and the model across three contrasts. Notice that direction biases are estimated from time 100 ms after pursuit onset for human tracking and time 140 ms for model output, to take into account the 40–50 ms lag introduced in the horizontal component of the model. The initial direction bias in the smooth pursuit responses was highest for low contrast (10%), reaching the oblique direction (45°, dotted horizontal line). It then decayed over time. Such initial bias was reduced with increasing contrast, as found previously with multiple edges objects (Wallace et al., 2005) (Fig. 9a and b). Model output successfully reproduced these effects about time course and contrast-dependency. However, when the initial directional error for the model was compared with that of the data obtained with subject AM, the initial directional bias values for the model was slightly higher for 30% and 90% contrast values and low directional bias for low contrast unlike what is observed with the data and the model performance for subject GM. This result was the only difference between observed and predicted values. This could be due to the significant directional anisotropies found for this particular subject (Fig. 5b) that are used to tune the model as well as the lower variances observed with blob and upright target (Fig. 2c) that are used as inputs to the model.

Table 1
Timing parameter values for the recurrent Bayesian model.

Subject	δt_{1d} (ms)	δt_{2d} (ms)	δt_{fb} (ms)
GM	20	50	65
AM	20	50	92

4. Discussion

In the present study, we attempted to explain the dynamics of motion integration in the context of smooth pursuit responses using a recurrent Bayesian model. Our model has two stages. The first stage is a sensory integration stage, implemented as a recurrent Bayesian loop and the second stage is an oculomotor plant. The model takes the initial independent likelihoods of ambiguous 1D information and unambiguous 2D information as input (for all times) and combines them with an updating prior thereby optimally integrating the motion information to obtain a coherent percept of object's global motion. The dynamic MAP of the first stage is fed into the oculomotor plant to produce the final output of the model.

Table 2
Best-fit parameters of the oculomotor plant model.

	Oculomotor plant (X)				Oculomotor plant (Y)					
	k_p		k_d		k_p		k_d		τ	
Condition (contrast and speed)	AM	GM	AM	GM	AM	GM	AM	GM	AM	GM
10% & 7°/s	10.66	13.74	0.22	0.07	6.56	9.88	0.26	0.05	82	80
30% & 7°/s	10.43	12.22	0.26	0.12	9.23	7.87	0.1	0.32	72	70
90% & 7°/s	9.93	13.22	0.30	0.09	8.35	9.66	0.23	0.07	62	60
100% & 5°/s	11.05	8.1	0.26	0.38	8.59	6.54	0.41	0.36	100	70
100% & 10°/s	10.12	7.89	0.31	0.42	8.22	6.51	0.40	0.37	100	70
100% & 15°/s	12.06	7.32	0.15	0.47	8.27	7.31	0.45	0.35	100	70

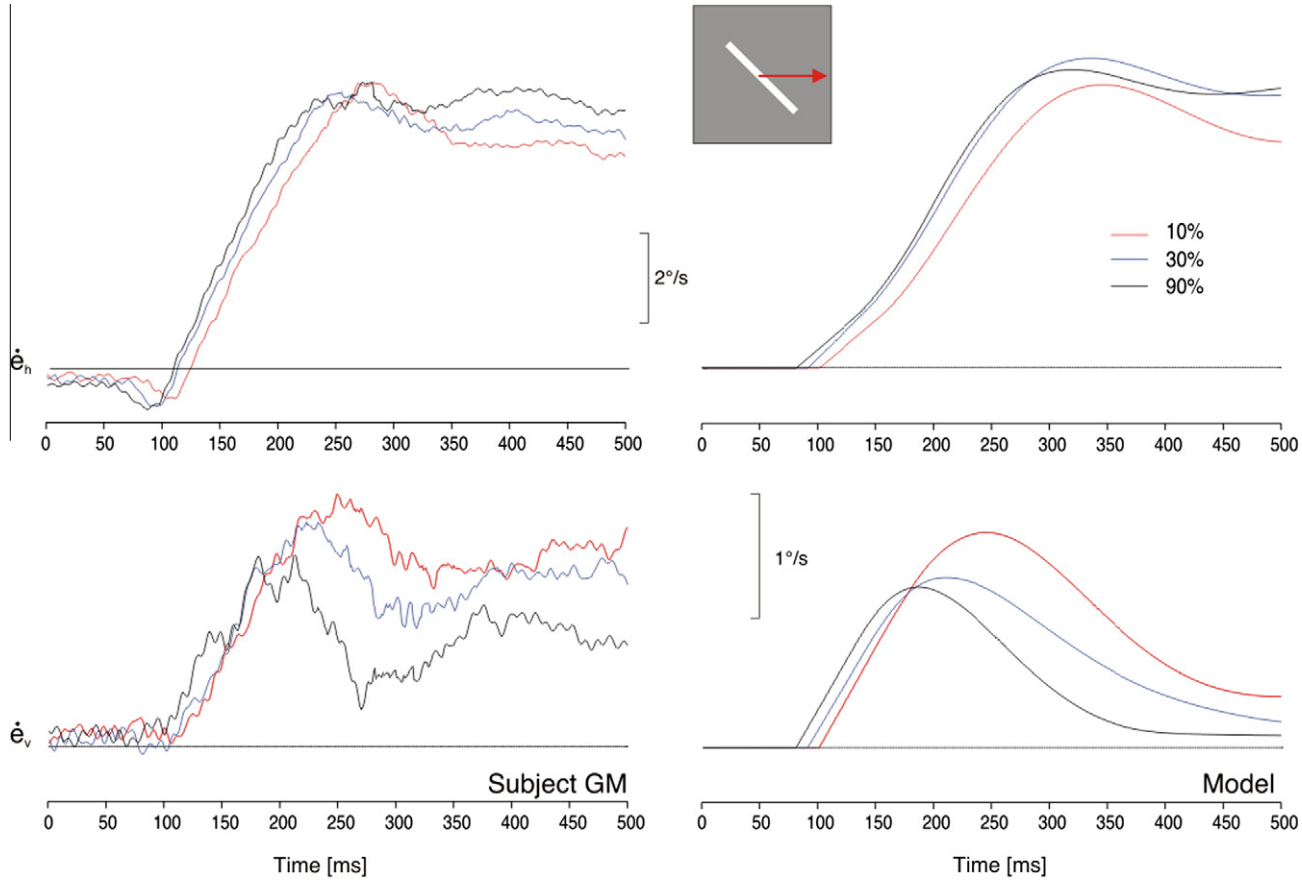

Fig. 7. Pursuit eye velocity traces for data and the model (varying *contrast).* Human (right column) and model (left column) responses to a tilted line (+45°) moving at 7°/s and presented at three different contrast (10%, 30% and 90%: red, blue and black curves, respectively). Curves are mean horizontal (horizontal $\dot{e}_h$) and vertical ($\dot{e}_h$) eye velocities.

Table 3
Root mean square deviation (deg/s) for the model output and mean smooth pursuit traces for a moving tilted line.

	Subject: AM		Subject: GM	
Contrast (%)	Horizontal component ($\dot{e}_h$)	Vertical component ($\dot{e}_v$)	Horizontal component ($\dot{e}_h$)	Vertical component ($\dot{e}_v$)
10	0.87	0.27	0.57	0.12
30	1.09	0.22	0.61	0.18
90	0.81	0.21	0.60	0.12

Such Bayesian framework has been successfully applied to model perceived motion direction and speed perception (Stocker & Simoncelli, 2006; Weiss et al., 2002). However, these earlier models depart from ours in three important aspects. First, they did not predict any significant bias at full contrast. Second, they were static models and did not try to account for the temporal dynamics of motion integration. Third, they did not consider all different motion information available from the images and thus ignored the role of 2D feature motions in the actual implementation of the model. Here, we extended this theoretical approach to a dynamic implementation, by recurrently updating the Prior knowledge with the Posterior at the end of each iteration. A model

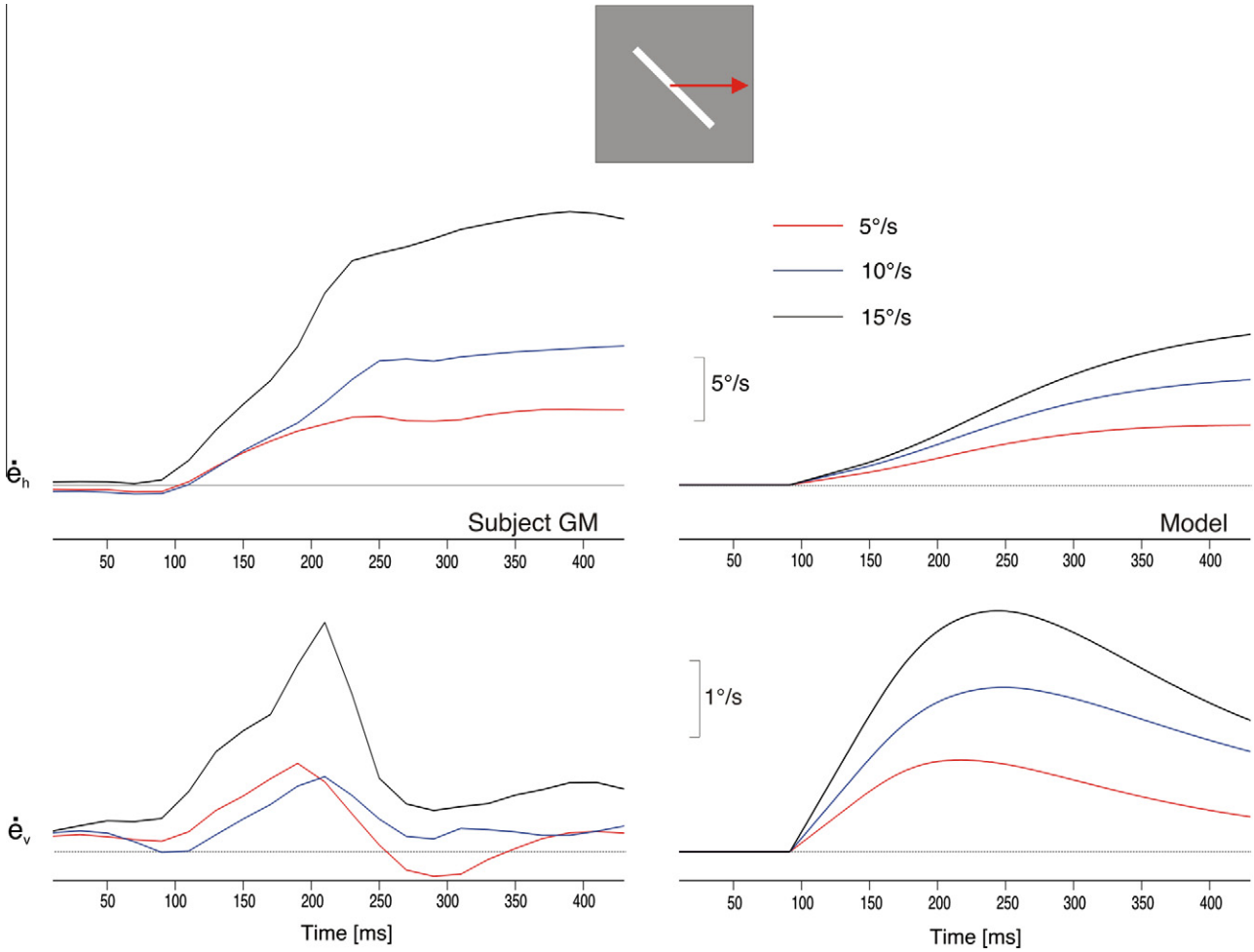

Fig. 8. Pursuit eye velocity traces for data and the model (varying speed). Human (right column) and model (left column) responses to a tilted line (+45°) moving at 7°/s and presented at three different speeds (5, 10 and 15°/s: red, blue and black curves, respectively). Curves are mean horizontal (horizontal $\dot{e}_h$) and vertical ($\dot{e}_v$) eye velocities.

describing the dynamic solution to the aperture problem is needed to explain the characteristic time course of eye movement velocity profiles while tracking, for instance a horizontally-moving tilted line. Our first attempt to implement a recurrent Bayesian model of motion integration (Montagnini et al., 2007) could not provide a complete account of the dynamic motion integration as observed in the oculomotor traces. The previous version of the model was limited to a qualitative description of the tracking direction error with arbitrary time scales, similar to a subsequent study by Dimova & Denham, 2009, reproducing our results. Here, we improved the Recurrent Bayesian model with an extension of oculomotor plant as a back end in order to produce realistic eye-velocity profiles reflecting the characteristic dynamics of motion integration. This model not only gives an accurate qualitative account of the motion integration dynamics but also a quantitative account that is closely comparable to the smooth pursuit responses for different speeds and contrasts.

The final output mimics the open-loop phase of smooth pursuit response to a horizontally-moving tilted line-stimulus. The choice to limit the model to the open-loop phase, allows us to avoid the computational complexity involved in updating the measurement likelihood functions (1D and 2D) during the closed loop phase when the oculomotor feedback is integrated in the smooth pursuit control. This recurrent Bayesian model is equivalent to a simple Kalman filter with a gain equal to 1 for the initial measurement that is the same for all iterations. Further work is needed to extend the current model to the closed-loop mode. This will need to include the effect of the positive feedback loop involved in maintaining steady-state pursuit (Goldreich et al., 1992; Miles & Fuller, 1975). One difficulty will then be to estimate the variance of such internal signal, building eye velocity likelihood or combining image motion or pursued target estimates (Freeman, Champion, & Warren, 2010) in head-centered coordinates.

A strong point of our approach is that the free parameters of the Bayesian distributions (the Prior, 1D- and 2D-likelihood's variance) are estimated from an independent set of oculomotor data. We assumed that smooth pursuit variance at the peak acceleration time for pure 1D and pure 2D stimulus was closely related to the 1D and 2D likelihoods. The results obtained with subject AM (Fig. 9) suggest that this method is not always accurate when rendering the effects of very low contrasts. Further work is needed to compare model outputs when estimating velocity likelihoods at different point in time since contrast is known to affect the intrinsic dynamics of motion processing, including latency and temporal dynamics of early visual neurons (Albrecht, Geisler, Frazor, & Crane, 2002). This would improve the model to give a better quantitative account of the dynamic motion integration that is closer to the smooth pursuit responses.

In the sensory integration stage, appropriate internal delays were introduced, independently for the 1D and 2D information

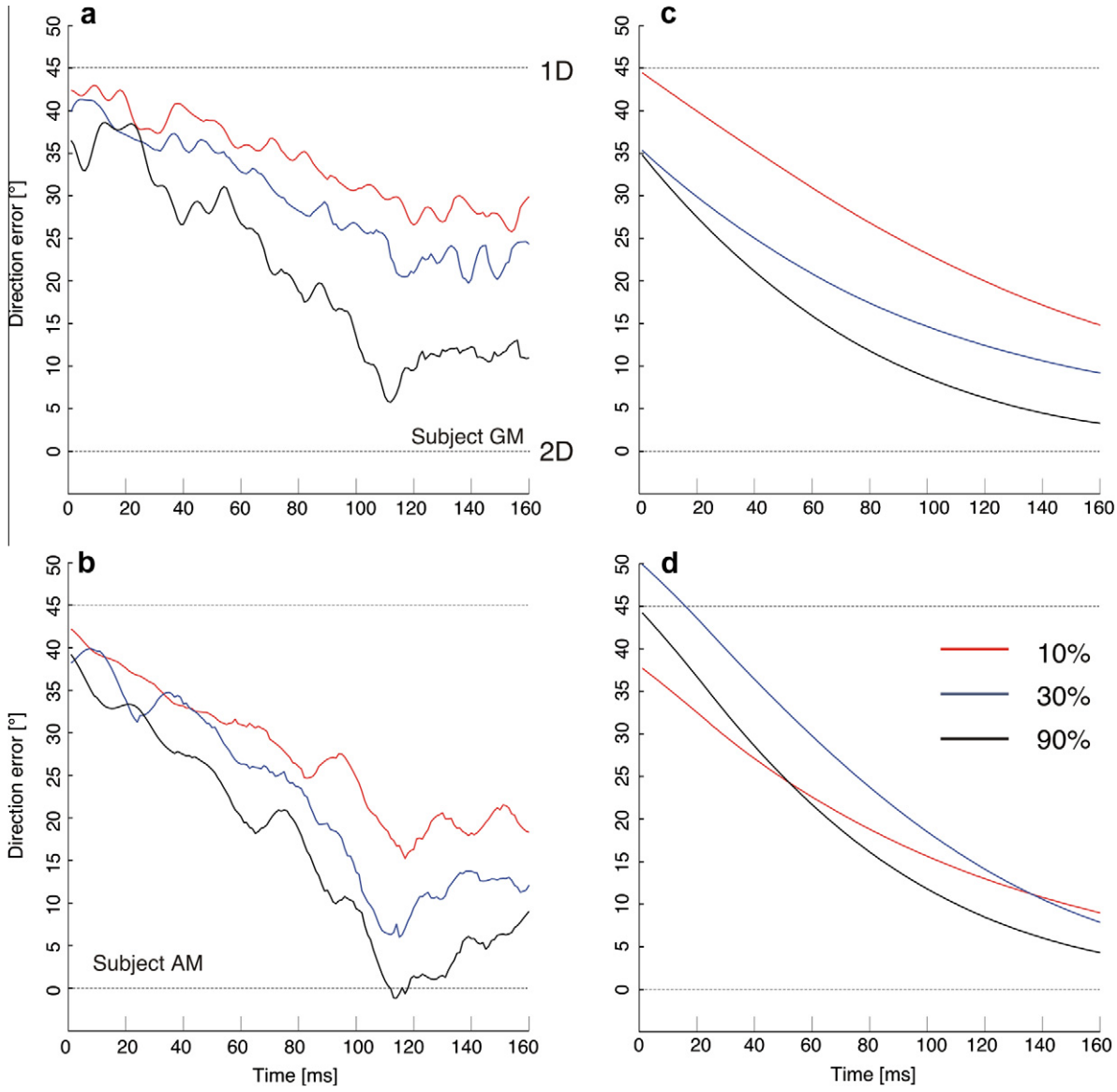

Fig. 9. Direction bias in data and the model (varying contrast). Tracking direction errors for two human subjects (left columns) plotted against time. Model responses obtained with parameters fitted for each subject with the data presented in Figs. 2–5 are plotted in the right columns. Model has been run for three different contrast values: 10% (red), 30% (blue) and 90% (black). Data are direction biases (i.e. atan ($\dot{e}_v/\dot{e}_h$)) measured from 100 and 140 ms after pursuit onset for human and model data, respectively, to account for the time lag of 40–50 ms introduced in the horizontal component of the model.

processing pathways, and they were chosen in such a way that the dynamics of the recurrent Bayesian MAP is comparable to the dynamics of MT neurons (Pack & Born, 2001). The time for the initiation of encoding the true global velocity of the stimulus (~70 ms) for the model is in agreement with the dynamics of motion signaling by neurons in MT (Smith et al., 2005; Pack et al., 2004). However, such additional delay introduced in 2D velocity likelihood computation slightly over-estimates the values obtained in human subjects with ocular following responses. Earlier work from our group showed that 2D-driven responses were delayed by about 20–30 ms relative to tracking onset driven by the 1D edges (Masson & Castet, 2002; Masson et al., 2000). Such delay increased to 40–50 ms with low contrast values. Moreover, the changes in both 1D- and 2D-driven responses observed with ocular following when lowering contrast is highly non-linear (Barthélemy et al., 2008). Further work will implement such non-linear effects to make the system dynamics more realistic across a large range of contrast or noise levels. The decay time constant (~65 ms) of the vertical component of MAP, for a horizontally-moving tilted line, was set in agreement with the time constant of the change in preferred direction as observed with a population of MT neurons (Pack & Born, 2001; see Fig. 1c) and results obtained at high contrast with tilted lines (Fig. 9) show that such values are in fact consistent with pursuit dynamics.

Finally, the gain parameters of the oculomotor plant were tuned with an independent set of data to incorporate both anisotropies and non-linearities that can be seen in human smooth pursuit oculomotor recordings. This is unlike previous oculomotor models that adopted a free parameter tuning strategy that would give a best fit of the model to the data, mostly along one direction only. Clearly, we need to better document the properties of smooth pursuit along oblique direction and more complex trajectories (e.g. DeSperati & Viviani, 1997; Soechting et al., 2005) in order to simulate pursuit to 2D motion trajectories. Another difficulty we encountered is the ability of the oculomotor plant model to respond to transient input such as the vertical component of the

MAP estimate with tilted lines. Transient changes in direction often occur in natural scenes. Moreover, as in the aperture problem, sensory estimate can quickly vary over time. MT neurons can follow these dynamics (e.g. Osborne, Bialek, & Lisberger, 2004; Pack & Born, 2001) and primate pursuit can cope with these (Osborne, Hold, Bialek, & Lisberger, 2007). However, we need to better model pursuit responses to these transient changes such as illustrated in MAP signals in Fig. 6.

To conclude, our two-stage model provides a novel approach to bridge the gap between a well-established theoretical framework like the Bayesian theory and the eye movement data, in modeling the transient behavioral dynamics. Importantly, this two stage framework can be extended to implement an independent perceptual mechanism operating on the posterior distribution of the recurrent Bayesian stage. In addition, decision rules other than MAP might be considered, possibly allowing us to take into account the posterior variance, instead of the mere maximum. Lastly, how different decision rules can better describe different data from the posterior distribution need to be investigated.

Acknowledgments

We are deeply thankful to F.V. Barthélémy for helping us in setting up the lab. ARB is funded by the CODDE ITN Network from the European Community's Seventh Framework Programme FP7/2007-2013 under grant agreement number 214728-2. AM was supported by the FACETS European IP Project (Sixth Framework, IST-FET-). We thank E. Castet and L. Goffart for their scientific advices in the building of the model and A. DeMoya, J. Baurberg and T. Iherti for their excellent technical support.

References

Albrecht, D. G., Geisler, W. S., Frazor, R. A., & Crane, A. M. (2002). Visual cortex neurons of monkeys and cats: Temporal dynamics of the contrast response function. *Journal of Neurophysiology, 88*, 888–913.

Barthélemy, F. V., Perrinet, L. U., Castet, E., & Masson, G. S. (2008). Dynamics of distributed 1D and 2D motion representations for short-latency ocular following. *Vision Research, 48*, 501–522.

Born, R. T., Pack, C. C., Ponce, C. R., & Yi, S. (2006). Temporal evolution of 2-dimensional direction signals used to guide eye movements. *Journal of Neurophysiology, 95*, 284–300.

Bradley, D. C., & Goyal, M. S. (2008). Velocity computation in the primate visual system. *Nature Reviews Neuroscience, 9*, 686–695.

Busettini, C., Miles, F. A., & Schwarz, U. (1991). Ocular responses to translation and their dependence on viewing distance. II. Motion of the scene. *Journal of Neurophysiology, 66*, 865–878.

Castet, E., Lorenceau, J., Shiffrar, M., & Bonnet, C. (1993). Perceived speed of moving lines depends on orientation, length, speed and luminance. *Vision Research, 33*, 1921–1936.

Collewijn, H., van der Mark, F., & Jansen, T. C. (1975). Precise recordings of human eye movements. *Vision Research, 15*, 447–450.

DeAngelis, G. C., & Uka, T. (2003). Coding of horizontal disparity and velocity by MT neurons in the alert macaque. *Journal of Neurophysiology, 89*, 1094–1111.

DeSperati, C., & Viviani, P. (1997). The relationship between curvature and velocity in two-dimensional smooth pursuit eye movements. *Journal of Neuroscience, 17*(10), 3932–3945.

Dimova, K. D., & Denham, M. J. (2009). A neurally plausible model of the dynamics of motion integration in smooth eye pursuit based on recursive Bayesian estimation. *Biological Cybernetics, 100*, 185–201.

Dimova, K. D., & Denham, M. J. (2010). A model of plaid motion perception based on recursive Bayesian integration of the 1-D and 2-D motions of plaid features. *Vision Research, 50*, 585–597.

Freeman, T. C., Champion, R. A., & Warren, P. A. (2010). A Bayesian model of perceived head-centered velocity during smooth pursuit eye movement. *Current Biology, 20*, 757–762.

Goldreich, D., Krauzlis, R. J., & Lisberger, S. G. (1992). Effect of changing feed back delay on spontaneous oscillations in smooth pursuit eye movements of monkeys. *Journal of Neurophysiology, 67*, 625–638.

Heinen, S. J., & Watamaniuk, S. N. J. (1998). Spatial integration in human smoothpursuit. *Vision Research, 38*, 3785–3794.

Hurlimann, F., Kiper, D. C., & Carandini, M. (2002). Testing the Bayesian model of perceived speed. *Vision Research, 42*, 2253–2257.

Kersten, D., Mamassian, P., & Yuille, A. (2004). Object perception as Bayesian inference. *Annual Review of Psychology, 55*, 10.1–10.32.

Krauzlis, R. J., & Miles, F. A. (1996). Initiation of saccades during fixation and pursuit: Evidence in humans for a single mechanisms. *Journal of Neurophysiology, 76*, 4175–4179.

Lisberger, S. G. (2010). Visual guidance of smooth-pursuit eye movements: Sensation, action, and what happens in between. *Neuron, 66*, 477–491.

Lorenceau, J., & Shiffrar, M. (1992). The influence of terminators on motion integration across space. *Vision Research, 32*, 263–273.

Lorenceau, J., Shiffrar, M., Wells, N., & Castet, E. (1993). Different motion sensitive units are involved in recovering the direction of moving lines. *Vision Research, 33*, 1207–1217.

Masson, G. S., & Castet, E. (2002). Parallel motion processing for the initiation of short-latency ocular following in humans. *Journal of Neuroscience, 22*, 5149–5163.

Masson, G. S., & Ilg, U. J. (2010). *Dynamics of visual motion processing: Neuronal, behavioral, and computational approaches*. New-York: Springer Verlag.

Masson, G. S., Rybarzcyk, Y., Castet, E., & Mestre, D. R. (2000). Temporal dynamics of motion integration for the initiation of tracking eye movements at ultra-short latencies. *Visual Neuroscience, 17*, 753–767.

Masson, G. S., & Stone, L. S. (2002). From following edges to pursuing objects. *Journal of Neurophysiology, 88*, 2869–2873.

Miles, F. A., & Fuller, J. H. (1975). Visual tracking and the primate flocculus. *Science, 189*, 1000–1003.

Montagnini, A., Mamassian, P., Perrinet, L. U., Castet, E., & Masson, G. S. (2007). Bayesian modeling of dynamic motion integration. *Journal of Physiology (Paris), 101*, 64–77.

Montagnini, A., Spering, M., & Masson, G. S. (2006). Predicting 2D target velocity cannot help 2D motion integration for smooth pursuit initiation. *Journal of Neurophysiology, 96*, 3545–3550.

Movshon, J. A., Adelson, E. H., Gizzi, M. S., & Newsome, W. T. (1986). The analysis of moving visual patterns. *Experimental Brain Research, 11*, 117–152.

Osborne, L. C., Bialek, W., & Lisberger, S. G. (2004). Time course of information about motion direction in visual area MT of macaque monkey. *Journal of Neuroscience, 31*, 3210–3222.

Osborne, L. C., Hold, S. S., Bialek, W., & Lisberger, S. G. (2007). Time course of precision in smooth – pursuit eye movements of monkeys. *Journal of Neuroscience, 27*(11), 2987–2998.

Osborne, L. C., Lisberger, S. G., & Bialek, W. (2005). A sensory source for motor variation. *Nature, 437*, 412–416.

Pack, C. C., & Born, R. T. (2001). Temporal dynamics of a neural solution to the aperture problem in visual area MT of macaque brain. *Nature, 409*, 1040–1042.

Pack, C. C., Gartland, A. J., & Born, R. T. (2004). Integration of contour and terminator signals in visual area MT of alert macaque. *Journal of Neuroscience, 24*(13), 3268–3280.

Pack, C. C., Hunter, J. N., & Born, R. T. (2005). Contrast dependence of suppressive influences in cortical area MT of alert macaque. *Journal of Neurophysiology, 93*(3), 1809–1815.

Rust, N. C., Mante, V., Simoncelli, E. P., & Movshon, J. A. (2006). How MT cells analyze the motion of visual patterns. *Nature Neuroscience, 9*(11), 1421–1431.

Simoncelli, E. P., Adelson, E. H., Heeger, D. J. (1991). Probability distribution of optical flow. In *Proceedings of the IEEE conference on computer and vision pattern recognition* (pp. 310–315).

Smith, M. A., Majaj, N. J., & Movshon, A. J. (2005). Dynamics of motion signalling by neurons in macaque area MT. *Nature Neuroscience, 8*, 220–228.

Soechting, J. F., Mrotek, L. A., & Flanders, M. (2005). Smooth pursuit tracking of an abrupt change in target direction: Vector superposition of discrete responses. *Experimental Brain Research, 160*, 245–258.

Spering, M., Kerzel, D., Braun, D. I., Hawken, M. J., & Gegenfurtner, K. R. (2005). Effects of contrast on smooth pursuit eye movements. *Journal of Vision, 5*, 455–465.

Stocker, A. A., & Simoncelli, E. P. (2006). Noise characteristics and prior expectations in human visual speed perception. *Nature Neuroscience, 9*, 578–585.

Tanaka, M., & Lisberger, S. G. (2001). Regulation of the gain of visually guided smooth-pursuit eye movements by frontal cortex. *Nature, 409*, 191–194.

Tlapale, E., Masson, G. S., & Kornprobst, P. (2010). Modeling the dynamics of motion integration with a new luminance-gated diffusion mechanism. *Vision Research, 50*, 1676–1692.

Tsui, J. M. G., Hunter, N., Born, R. T., & Pack, C. C. (2010). The role of V1 surround suppression in MT motion integration. *Journal of Neurophysiology, 103*(6), 3123–3128.

Wallace, J. M., Stone, L. S., & Masson, G. S. (2005). Object motion computation for the initiation of smooth pursuit eye movements in humans. *Journal of Neurophysiology, 93*, 2279–2293.

Wallach, H. (1935). Visual truth movement directions. *Psychologie Forshung, 20*, 325–380.

Weiss, Y., & Adelson, E. (1998). Slow and smooth: a Bayesian theory for the combination of local motion signals in human vision. *MIT technical report*, A.I. Memo 1624.

Weiss, Y., Simoncelli, E. P., & Adelson, E. H. (2002). Motion illusions as optimal percepts. *Nature Neuroscience, 5*, 598–604.